

Heat conduction in a two-dimensional Ising model

M. Casartelli^{1,2,3,a}, N. Macellari¹, and A. Vezzani^{1,2}

¹ Dipartimento di Fisica, Università di Parma, Viale Usberti 7/A (Parco Area Scienze) 43100 Parma, Italy

² CNR-INFM (Parma), Viale Usberti 7/A (Parco Area Scienze) 43100 Parma, Italy

³ INFN, gruppo collegato di Parma, Viale Usberti 7/A (Parco Area Scienze) 43100 Parma, Italy

Received 25 October 2006 / Received in final form 17 January 2006

Published online 12 April 2007 – © EDP Sciences, Società Italiana di Fisica, Springer-Verlag 2007

Abstract. A cylindrical Ising model between thermostats is used to explore the heat conduction for any temperature interval. The standard Q2R and Creutz dynamics, previously used by Saito, Takesue and Miyashita, fail below the critical temperature, limiting the analysis to high temperatures intervals. We introduce improved dynamics by removing limitations due to the chessboard-like refresh, and by supplementing the Q2R rule with Kadanoff-Swift moves. These new dynamics not only prove highly efficient in recovering old results in their domains of validity, but also allow exploration of steady heat transport between two arbitrary temperatures, i.e. very far from equilibrium. From an ansatz avoiding references to quasi equilibrium or to local temperature, and from comparison with numerical simulations, we can consistently define a generalized diffusivity. Its dependence on the energy density may be evaluated without any recourse to the Green-Kubo formula.

PACS. 05.60.-k Transport processes – 05.50.+q Lattice theory and statistics (Ising, Potts, etc.) – 44.10.+i Heat conduction

1 Introduction

In studying non-equilibrium properties, much attention has been devoted to heat transport phenomena in terms of microscopic dynamics, checking the validity of Fourier's Law, or looking at reasons for its possible failure. Anomalies have been noticed recently and discussed, for instance, in Hamiltonian nonlinear systems (see [1] and references therein). We recall that, according to the phenomenological Fourier's Law, for a macroscopic system in a steady state the heat flow is proportional to the temperature gradient. This behavior is generally postulated for quasi equilibrium states, where a local temperature exists. However, a steady state may be defined also far from equilibrium, as a state whose relevant mean properties are translationally invariant in time.

Focusing on magnetic systems, most recent works stress the one dimensional case for various models (e.g. [2–5]). For two dimensional models, the literature is sparse, despite the fact that such systems seem to be more interesting. This is not only because they give realistic properties in modelling real systems, but also conceptually, for the additional problems opened by the existence of critical phenomena.

A cylindrical Ising model, i.e. a ferromagnetic square lattice, with two borders at temperatures T_1 and T_2 in one direction and periodic conditions in the other, has

been studied for instance by Saito, Takesue and Miyashita (STM) using Creutz and Q2R dynamics [6]. They show that the conductivity at temperature T obtained through the Green-Kubo formula is in good agreement with direct measures of heat transfer when an infinitesimal temperature gradient is applied to the borders ($T_1 = T$ and $T_2 = T + \delta T$). In their investigations, a severe obstacle arises from the failure of Q2R and Creutz dynamics below the critical temperature T_c , where the system behaves as if the conductivity were zero. Therefore, Fourier's Law has been successfully checked only for $T > T_c$. However, transport phenomena also occur at low temperatures and far from equilibrium. In particular, it is likely that anomalies could appear in the range $T_1 < T_c < T_2$, with the coexistence of different magnetic phases and with related problems for interfaces, which have so far been completely ignored. Therefore, in order to realistically simulate the whole range of temperatures, another form of dynamics is required.

In the present paper we shall introduce such an alternative dynamic model in two steps: (1) by substituting a random update to the usual parallel refresh; (2) by supplementing the Q2R rule with a second-neighbours move suggested, in another context, by Kadanoff and Swift [7]. After checking the full consistency with previous results at high temperatures, the new dynamics will be shown to lead to meaningful simulations for *every* temperature interval $0 \leq T_1 \leq T_2 \leq \infty$. We study the profile of energy

^a e-mail: casartelli@fis.unipr.it

densities along the direction of the temperature gradient showing that our results are consistent with the Fourier equation with a temperature dependent diffusivity.

The paper is organized as follows. In Section 2 we present the model with old and new dynamics. In Section 2.2 we consider random Q2R, showing, in particular, that in the one dimensional system this first step alone is sufficient to cancel spurious ballistic effects, leading to the correct conduction law (exact probabilistic calculations are given in Appendix A). On the other hand, we show that for the cylinder non-ergodic behaviour at low temperature is still present. Moreover, we clarify some thus far overlooked aspects and consequences of non-ergodicity at low energy. In Section 2.3 the new dynamics are presented, stressing on their conceptual and numerical advantages. Numerical experiments on diffusion and transport are reviewed in Section 3, with a systematic comparison between equilibrium and non-equilibrium distributions (Sect. 3.1). For a more conceptual interpretation, in Section 3.2 we show that our results are consistent with the Fourier approach rewritten in terms of energy density. Moreover, from the energy distribution obtained in our simulations, we can directly derive the behaviour of diffusivity vs. energy, avoiding the Green-Kubo formula. We show that the diffusivity tends to 0 at T_c in the thermodynamic limit, which is expected since diffusivity is the ratio between conductivity and specific heat.

2 Conservative evolution rules at all energies

2.1 The cylindrical Ising model

The model considered by STM consists of a $L \times L$ square lattice, with periodic conditions in the y direction and open boundaries in the x direction, i.e. a *cylindrical* square lattice. In every site the spin variable $\sigma_{x,y}$ assumes values 1 or -1 . Adjacent spins with opposite values give an energy unit to the system. The normalized total energy E_{tot} is therefore:

$$E_{tot} = \frac{1}{4L^2} \sum_{x,y} \sum_{\langle x,y \rangle} \frac{1 - \sigma_{x,y} \sigma_{\langle x,y \rangle}}{2} \quad (1)$$

where $\langle x,y \rangle$ are the nearest neighbors of the site (x,y) .

The left and right boundaries are in contact with two thermostats. In order to simulate such devices, two supplementary columns have been added at each of the borders, and the sites of such columns evolve with the usual equilibrium Metropolis algorithm, i.e. their flip probability is

$$P(\Delta E) = P(-\Delta E)e^{-\Delta E/KT},$$

where ΔE is the energy variation due to the flip and K is the Boltzmann's constant (here $K = 1$). Interacting with such thermostats, fixed at $T = T_1$ and $T = T_2$ respectively, the cylinder can exchange energy through the borders. Apart from this contact, energy is conserved, therefore all internal sites must evolve according to an energy preserving (microcanonical) rule.

The simplest and traditional answer to the requirement of an energy preserving evolution for internal sites is the Q2R rule, introduced in 1984 by Vichniac (see e.g. [8–10]):

Q2R rule: in every site the spin is forced to flip whenever energy is preserved, i.e. when half the spins in the neighborhood are up and half are down.

Such moves are usually applied in a parallel way and, in order to avoid interferences, sites are updated along a chessboard scheme. A “time step” consists therefore of two semi-steps of $L^2/2$ simultaneous moves, on the even and the odd sublattices respectively. However, as recalled in the Introduction, Q2R does not work for low energy densities, when most of the spins are aligned with small spots in the opposite direction. Such spots are fixed or constrained to short periodical motions, without any possibility of carrying energy through the lattice, as if conductivity were zero. Moreover, final states strongly depend on the initial conditions, and orbits cannot explore the fixed-energy subset of the configuration space: in other words, the system is not ergodic. Problems arise just below the mean energy corresponding to $T = T_c$. In the present units, $T_c \simeq 2.27$, and parallel computations performed by STM block at around $T = 2$. The Creutz rule (which will not be considered in the present paper) does not eliminate this inconvenience.

For a chosen interval $[T_1, T_2]$, after reaching the steady state, the typical quantity to consider is the mean energy density $\langle E(x) \rangle$, where x is the column label (this requires of course both time and column average for each x). Such energy distributions $\langle E(x) \rangle$ may be plotted vs. x/L in order to compare systems of different sizes.

2.2 Random update

We observe that there are no intrinsic or physical reasons for the chessboard-like parallel update. More likely, the localization of possible flips could be influenced by small random perturbations. Our first improvement consists therefore in altering the order of Q2R moves: instead of the chessboard refresh, sites will be serially updated in a random order. A “time step” τ is defined as a sequence of L^2 random choices. For brevity, this “random order” rule will be denoted RQ2R.

Further support for the choice of random updates comes from the one dimensional case, where the alternate odd-even refresh implies a uniform “ballistic” motion of the spin variations (i.e. units of energy) along the chain. As a consequence, every site has the same energy on the average. Such a uniformity, independent of T_1 and T_2 , seems to be quite unphysical. Now, by using random update, one rapidly reaches a steady state where the spatial distribution of energies in the x direction is perfectly linear (see Fig. 1). This behaviour is consistent with a diffusive behaviour of the energy and with Fourier's Law with constant diffusivity. We remark that the one dimensional lattice is very peculiar, since Fourier's Law may be exactly recovered by looking at the microscopical evolution of the link energies. Such a calculation is given in Appendix A.

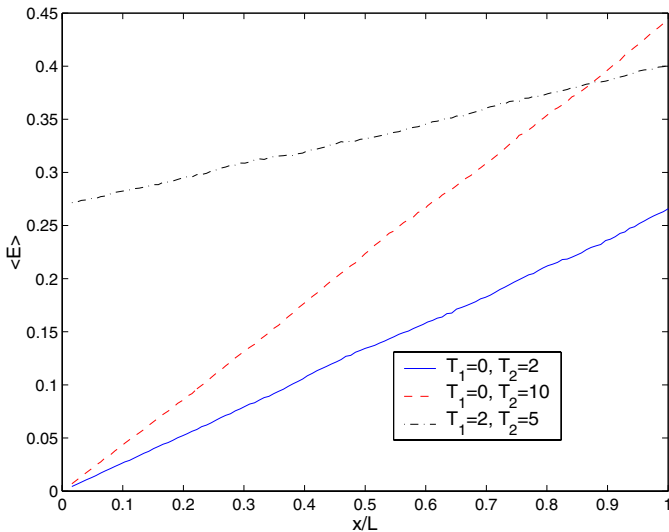


Fig. 1. The average energy density as a function of the site position, for the 1-dimensional system with size $L = 128$ and three temperature intervals. Averages run over 10^6 time steps. On the borders the energies are given by the equilibrium values $E_{eq}(T_1)$ and $E_{eq}(T_2)$.

In the two dimensional case, the passage to random update is still not sufficient for a full dynamization of typical low energy configurations. We shall report here a number of experiments illustrating the conductivity breakdown. This review is interesting in itself, and it will also be useful for comparison with the improved dynamics of the next sections. The likely reason why STM have overlooked these situations consists in the fact that they focus on the Green-Kubo formula, or equivalently on infinitesimal difference in temperature, while most interesting non ergodic effects are present for $T_1 < T_c < T_2$.

An initial way to control the conductivity breakdown is to give a common temperature $T_1 = T_2 \equiv T_{12}$ to the thermostats, and observe whether the system reaches an equilibrium state corresponding to the temperature T_{12} . For $T_{12} > T_c$, no problem arises: Figure 2 shows that each row has on average the same energy as the canonical equilibrium distribution. Around T_c there is a dramatic increase of the relaxation time, and just a little below T_c the cylinder becomes non-conducting. The discontinuous energy profile is a clear signal of this behaviour. Indeed, if the system were a conductor, we would expect that, due to heat exchanges, all the rows would have the same energy on average. Finally, low temperature energy profiles, such as those in Figure 2, depend on the initial conditions and, starting with a uniform configuration ($T = 0$), the system would not evolve at all. Such a behavior is a rough but clear proof of the expected non-ergodicity.

The influence of the initial configuration is also evident in the more complex case with two temperatures, $T_1 < T_c < T_2$ (Fig. 3). Starting from a low temperature configuration, all is frozen and there is no heat exchange between different rows. On the other hand, starting from a random configuration (as we shall do from now on, unless otherwise stated), the heat flows. Energy profiles for

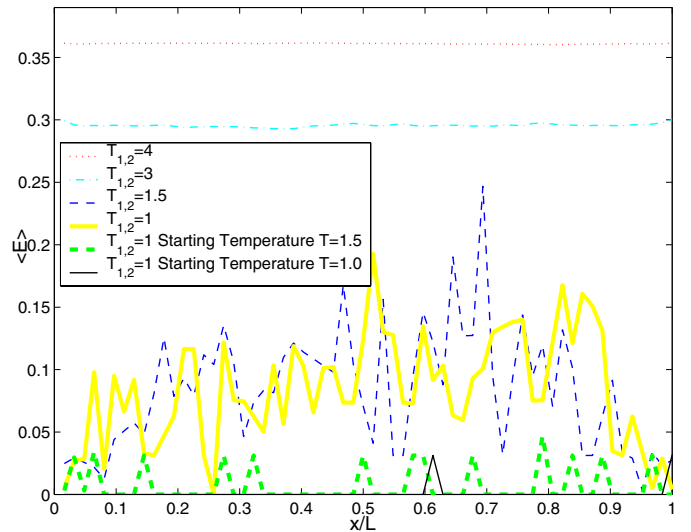


Fig. 2. Average energy profiles when borders are fixed at the same temperature T_{12} . Different behaviour is observed at high and low temperatures. For low temperature there is also evidence of a strong dependence on the starting configuration. In all figures, unless stated differently, the initial configuration is chosen at random, i.e. $T = \infty$.

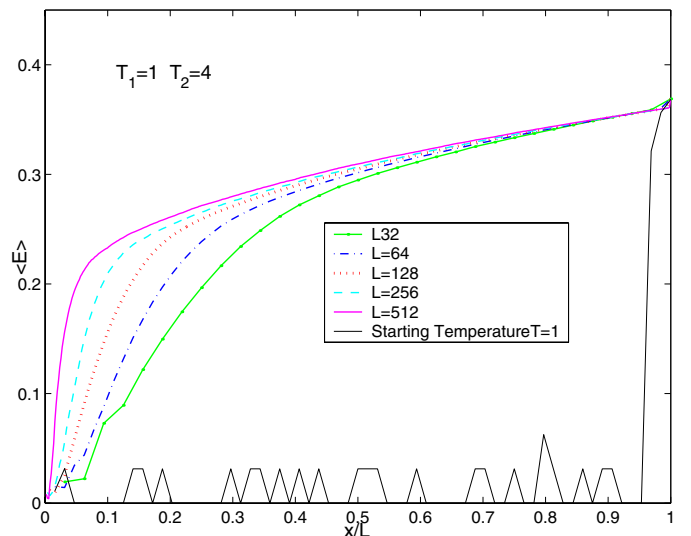


Fig. 3. Average energy profiles when the border temperatures are fixed to $T_1 = 1$ and $T_2 = 4$. The energies are obtained by averaging over 10^7 time steps. Different behaviour may be observed for different length and starting conditions.

growing L are shown in Figure 3. The presence of a thin conducting layer near the cold thermostat is obviously essential to keep a gradient of energy density in the x direction. The profile crossover, as L grows, may suggest that the thickness of such last layer depends on the rule and the temperature, but not on L . The existence of such a thin conducting layer for every $T_1 > 0$, at least when starting from a high temperature, is a remarkable effect. It shows that heat transport is possible even if one of the borders is at a temperature where the conductivity would be defined as zero: the apparent paradox is due to the fact that, as

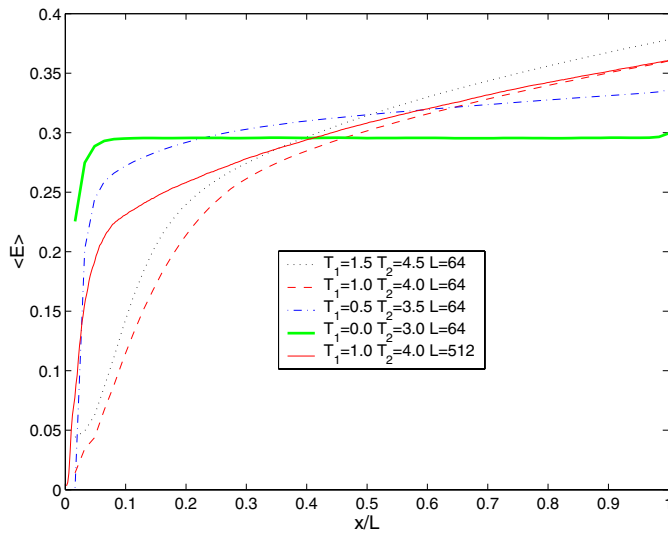


Fig. 4. The average energy density profiles for different border temperatures and system sizes. The energies are obtained by averaging over 10^7 time steps.

recalled in the Introduction, conductivity in this “static” sense is calculated in the situation when $T_2 = T_1 + \delta T$, and $\delta T \rightarrow 0$, giving zero indeed for $T_1 < T_c$. Yet, also for such a case, we verified that heat conductivity vs. size scales in a normal way, i.e. as expected in 2-dimensional systems, by fixing other parameters the energy transfer is independent of the system size. As suggested by Figure 4, if T_1 is lowered the probability of conducting events on the cold border decreases. Consistently, at $T_1 = 0$, all is frozen on the cold side: indeed in this case the energy distribution along the cylinder is flat, therefore there is no energy gradient and the heat transport vanishes as if the cold barrier were an insulator.

2.3 The Kadanoff-Swift move

In a different context, Kadanoff and Swift (KS) introduced a “magnetization preserving” microcanonical rule using a second-neighbor move [7].

KS move: consider a diagonal with two opposite spins, and exchange them whenever this exchange preserves the energy.

As a matter of fact, the conservation of magnetization is not required in this current study, but KS and Q2R moves can cooperate resolving local stalls: this means that sites and diagonals will be randomly chosen, alternating KS and Q2R rules, and a cycle of L^2 moves will constitute a single time step τ . This new energy-preserving dynamic model will be denoted KQ, by contracting KS and Q2R. It proves highly efficient in the dynamization of low energy situations, both in terms of a faster relaxation to the steady state and of activation of otherwise frozen phases.

The reliability of this KQ dynamic method can be checked by some obvious tests:

1. for *every* temperature T_{12} , putting $T_1 = T_2 = T_{12}$ we expect to relax to the equilibrium state equivalent to

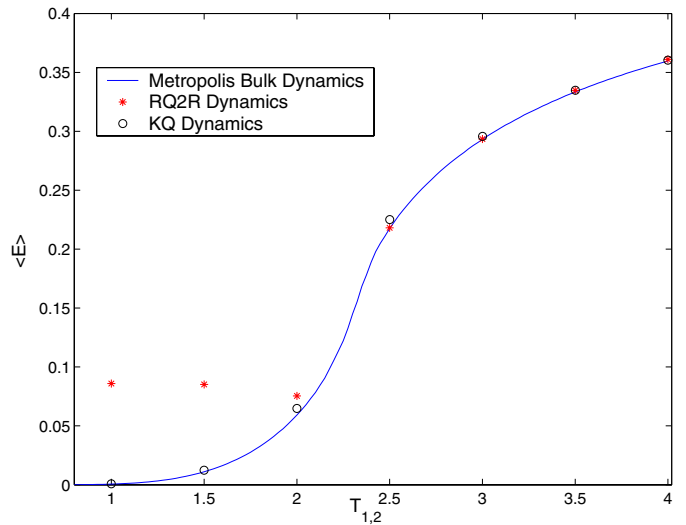


Fig. 5. The average energy of the system considering the standard bulk Metropolis dynamics, the RQ2R and the KQ dynamics for different temperatures $T_1 = T_2 = T_{12}$ the bulk dynamics have been performed with the whole system at temperature T_{12} .

the usual Ising-Metropolis model at the same temperature T_{12} . This indeed happens, with KQ dynamics, in the whole range of temperatures as illustrated in Figure 5, proving the effectiveness of the thermal contact with the thermostats (unlike the severe restrictions for previous rules). Moreover, the energy distribution along the cylinder is uniform on average.

2. in all cases, there is independence of initial conditions. In particular, it is possible to warm up an initially cold state, which is substantially more realistic than in previously considered dynamics.
3. unlike RQ2R, for the KQ dynamics there is heat-transport for any $[T_1, T_2]$, including the case of $T_1 = 0$. Moreover, the energy density profile is size independent even if $T_1 < T_c < T_2$, apart from possible finite size effects relevant at the critical energy. These properties are illustrated in Figure 6, where the average energy density profiles, for $T_1 = 0$ and $T_2 = 4$, are plotted for different system sizes.
4. starting from a random configuration, the transient before the steady state should be longer for lower temperatures at fixed dynamics, and faster in general for the KQ with respect to other dynamics. This is true. Actually, taking for instance $L = 64$, with $T_1 = 1$, $T_2 = 4$, a typical transient time is 10^3 steps for KQ, and 10^5 for RQ2R.
5. for $T_c < T_1 < T_2$, all should be the same (at least qualitatively) with all the rules, as it is. In this case indeed we always obtain a linear behaviour (constant diffusivity) as commented in Figure 7.

In conclusion, all tests agree on the reliability of KQ dynamics as an efficient alternative to previously considered rules, with a substantially larger domain of application.

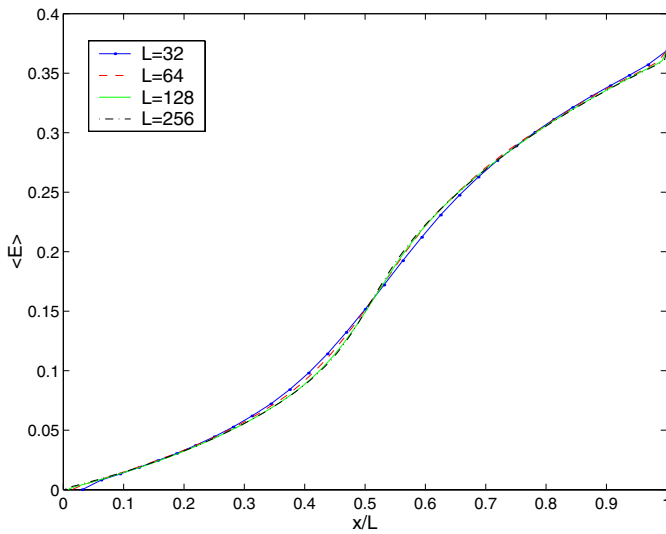


Fig. 6. The average energy density profiles for different system sizes. The energies are obtained averaging over 10^5 time steps.

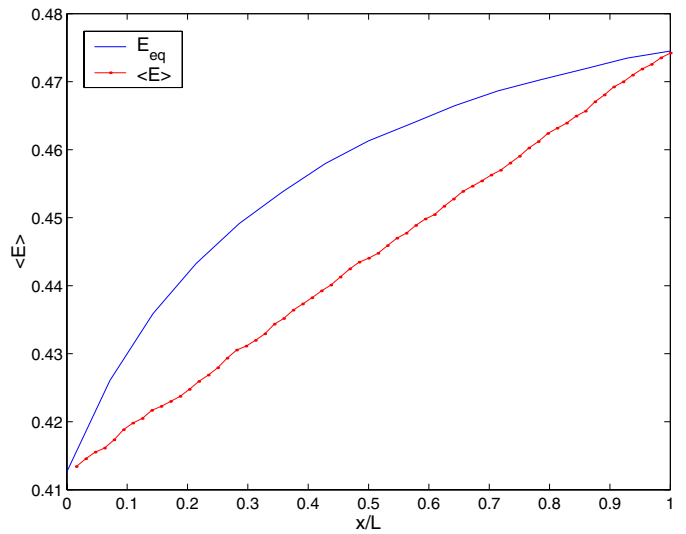


Fig. 7. The average energy density profiles when $T_1 = 6$ and $T_2 = 20$. The system size is $L = 64$ and the energies are obtained averaging over 10^5 time steps.

3 Numerical experiments

3.1 Staying far from equilibrium

Consider the standard periodic Ising-Metropolis lattice at equilibrium. For every temperature T , one can obtain the corresponding mean energy density $E_{eq}(T)$. The simplest curve which can be compared to the energy distribution profile is the distribution that one would get if the system were at local equilibrium and the temperature diffuses uniformly with constant conductivity. In this hypothesis the temperature would increase uniformly from T_1 to T_2 along the cylinder, and for each site one could consider the energy $E_{eq}(x)$, where E_{eq} is the equilibrium energy corresponding to the temperature T assigned to the site x . Of course, such a hypothesis is an oversimplification, however the energy profiles $E_{eq}(x)$ may constitute a reference frame for comparisons.

In all cases, by construction, the spatial profile $\langle E \rangle$ passes at the extremes $\bar{E}_{eq}(T_1)$ and $\bar{E}_{eq}(T_2)$, but the intermediate distributions strongly depend on the temperature interval. In particular, when T_1 is also much greater than T_c , $\langle E(x) \rangle$ is almost linear (see Fig. 7). As noticed in the one dimensional case, this linear behaviour corresponds to a uniform heat diffusion, with a diffusivity independent of $\langle E \rangle$. We note that, due to the non-constant specific heat, the uniform diffusion of the energy does not correspond to a uniform diffusion of the temperature. On the contrary, when T_c lies within the interval $[T_1, T_2]$, the spatial profile is more complicated (Fig. 8), and the simple picture of a uniform diffusion for temperature or energy does not work. A more general and effective framework will be discussed in the next subsection.

An interesting insight is offered by focusing on the cylinder configurations (Fig. 9), where a structured distribution of clusters is clearly detectable around the critical energy, just between the “chaotic” homogeneous grey of high energies or temperatures (magnetization $M = 0$)

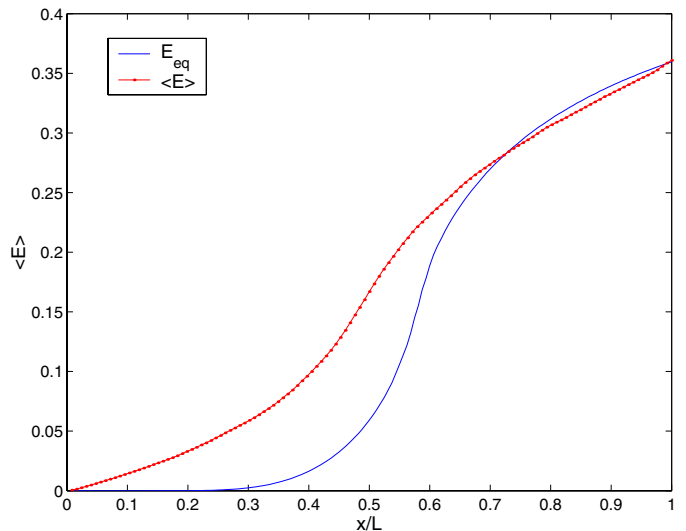


Fig. 8. The average energy density profiles when $T_1 = 0$ and $T_2 = 4$ compared with equilibrium distribution. The system size is $L = 128$ and the energies are obtained averaging over 10^5 time steps.

and the increasingly black (or white) configurations of low energies ($|M| > 0$, up to 1). The statistical problem of interfaces will be treated in a subsequent paper. We only observe here that this configurational transition takes place around $E(T_c)$, as expected, independently of the applied extreme temperatures. Thus, by lowering the difference $T_2 - T_1$ (always with $T_1 < T_c < T_2$) all goes as if we performed a zoom in the region around T_c . In other terms, there is an effective continuity in the configurational behavior of the system, observed by comparing what happens by lowering $T_2 - T_1$ at constant L and by enlarging L at constant $T_2 - T_1$.

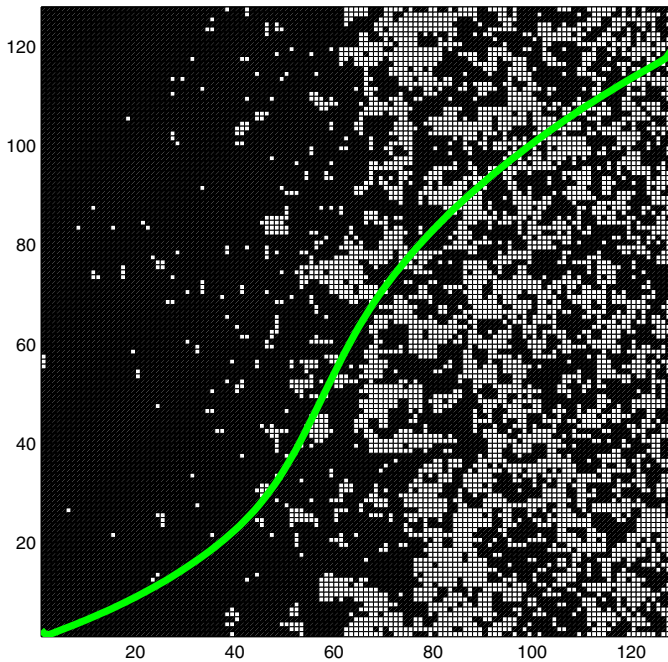


Fig. 9. A spin configuration, for size $L = 128$ and borders fixed at $T_1 = 1$ and $T_2 = 5$. The line between represents (in arbitrary units) the growth of the average energy along the cylinder.

3.2 Fourier's law and diffusivity

The discrepancy of energy profiles with respect to the equilibrium distribution suggests the presence of non trivial transport properties with a possible dependence of the local conductivity (and diffusivity) on the energy.

We return therefore to Fourier's empirical transport assumption from the very beginning, in terms of the heat flow through an elementary block. Usually, at quasi-equilibrium (required in order to speak of a local temperature), the minimal assumption is that the flowing heat energy per unit area is proportional to the temperature gradient ∇T via a proportionality constant κ (conductivity). This constant depends in principle on the energy density and in a non homogeneous model, on the spatial coordinates, through a matter density function ρ . This makes the assumption extremely general. Moreover, the usual conditions leading to Fourier's equation read

$$\rho \frac{\partial E}{\partial t} = \frac{\partial}{\partial x} \left(\kappa \frac{\partial T}{\partial x} \right) + \frac{\partial}{\partial y} \left(\kappa \frac{\partial T}{\partial y} \right) + \frac{\partial}{\partial z} \left(\kappa \frac{\partial T}{\partial z} \right). \quad (2)$$

As for the one dimensional array in Appendix A, we shall insist for notational convenience on the differential symbolism, even if our case is crudely discrete. Actually, conduction is one dimensional, the only gradient variable is x , and the minimal x is the lattice step. The cylinder is homogeneous, and we may assume $\rho = 1$ everywhere. Therefore, κ can depend on E , but not explicitly on x . As to a minimal time, it depends on the dynamical rule. Remembering that our time unit is $\tau = L^2$ moves, on a time scale t much greater than τ the true observable is the mean

energy density $\tilde{E}(x, t)$, i.e. E spatially averaged in the y direction, and time averaged for a number of moves of the order of some τ . Since these average operations are linear, we can write:

$$\frac{\partial \tilde{E}}{\partial t} = \frac{\partial}{\partial x} \left(\kappa \frac{\partial T}{\partial x} \right), \quad (3)$$

but

$$\frac{\partial E}{\partial x} = \frac{\partial E}{\partial T} \frac{\partial T}{\partial x} \Rightarrow \frac{\partial T}{\partial x} = \frac{\partial \tilde{E}}{\partial x} \bigg/ \frac{\partial \tilde{E}}{\partial T}$$

therefore

$$\frac{\partial \tilde{E}}{\partial t} = \frac{\partial}{\partial x} \left(\frac{\kappa}{C} \frac{\partial \tilde{E}}{\partial x} \right) \quad (4)$$

where $C = \partial \tilde{E} / \partial T$ is the specific heat: this still assumes the existence of a local temperature T . We can eliminate the variable T , relying exclusively on the real observable \tilde{E} :

$$\frac{\partial \tilde{E}}{\partial t} = \frac{\partial}{\partial x} \left(D(E) \frac{\partial \tilde{E}}{\partial x} \right). \quad (5)$$

In a quasi equilibrium state, (5) is equivalent to (4), i.e. to the standard Fourier's equation. However, since T does not appear in (5), and \tilde{E} is a well defined observable in every state, it may be read as an ansatz on the diffusion in very general conditions, independently of the existence of a local temperature. The function $D = D(E)$ is a diffusivity factor, recovering the normal diffusivity $D = \kappa / C$ in standard conditions.

Equation (5) can be introduced in an alternative way, avoiding from the very beginning the concept of local temperature. Let us consider a surface located at x_1 , dividing the cylinder into two regions. Let Q be the amount of energy crossing this surface so that $\partial Q / \partial t$ represents the heat flux. A reasonable hypothesis is that

$$\frac{\partial Q}{\partial t} = -D(E) \frac{\partial \tilde{E}}{\partial x}. \quad (6)$$

Equation (6) simply states that the heat flows from the side of the surface with highest energies to the side of lowest energy and the heat flux is proportional to the energy gradient. At this point, $D(E)$ is a proportionally constant depending only on the average energy of the surface. Let us consider two surfaces located in x_1 and in x_2 , one has:

$$\begin{aligned} \int_{x_1}^{x_2} \frac{\partial E}{\partial t} &= \frac{\partial Q}{\partial t} \bigg|_{x_1} - \frac{\partial Q}{\partial t} \bigg|_{x_2} \\ &= D(E) \frac{\partial \tilde{E}}{\partial x} \bigg|_{x_2} - D(E) \frac{\partial \tilde{E}}{\partial x} \bigg|_{x_1} \\ &= \int_{x_1}^{x_2} \frac{\partial}{\partial x} \left(D(E) \frac{\partial \tilde{E}}{\partial x} \right) \end{aligned} \quad (7)$$

since equation (7) holds for arbitrary x_1 and x_2 we obtain equation (5).

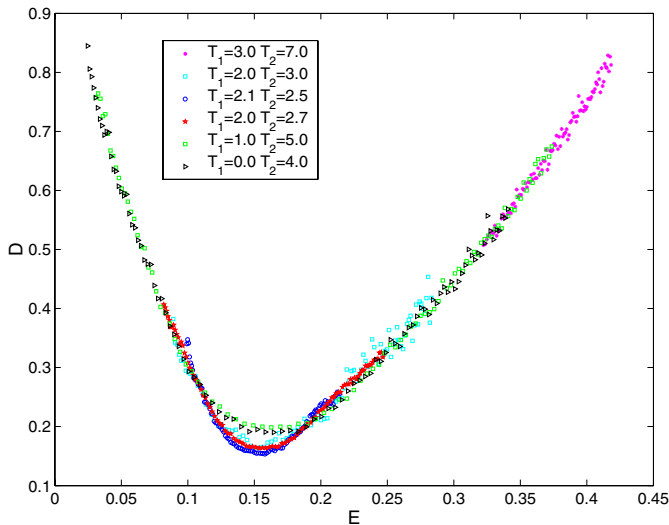


Fig. 10. Diffusivity evaluated by means of equation (8). The constant γ , in each interval, is obtained from equation (9) by calculating the heat absorbed per unit of time by the thermostat at temperature T_1 . Data refer to several temperature intervals, for $L = 128$ and averages over 10^5 – 10^6 time steps, depending on the temperature interval.

Now, in the steady state $\partial \tilde{E} / \partial t = 0$, therefore from (5) we have

$$\frac{\partial}{\partial x} \left(D(E) \frac{\partial \tilde{E}}{\partial x} \right) = 0, \quad \Rightarrow \quad D(\tilde{E}) = \frac{\gamma}{\partial \tilde{E} / \partial x}. \quad (8)$$

The last term in (8) can be calculated numerically, by looking for the derivative of the stationary quantity $\tilde{E}(x, t) = \langle E(x) \rangle$, as it results from dynamical simulations. The constant γ can be evaluated from the heat flux through a surface. Indeed from (6) and (8) we have

$$\gamma = \frac{\partial Q}{\partial t}. \quad (9)$$

In the stationary state the flux does not depend on the surface position along the cylinder, so that one can evaluate γ , for example, from the energy absorbed per unit of time by the thermostat. The value of γ and $D(E)$ are defined apart from an overall multiplicative factor, depending on the arbitrary definition of the timescales. However, once the convention on the timescale is fixed, by looking at the results obtained from different temperature intervals $[T_1, T_2]$, one should obtain consistent diagrams of $D(E)$ vs. E . This is indeed the case, as shown in Figure 10. The nice superposition of data relevant to different temperature intervals is a strong proof of the above picture of a heat flux with an energy dependent diffusivity. The function $D(E)$ presents a minimum at the critical energy $E_{eq}(T_c) \simeq 0.15$. We note that, since the specific heat C diverges at T_c in the thermodynamic limit, D should vanish at the critical point, therefore the measured finite value should be a finite size effect. This behaviour can indeed be inferred from our data: the value of the minimum decrease as the difference between T_1 and T_2 becomes smaller, and

this is equivalent (as remarked at the end of Sect. 3.1) to increasingly larger values of L .

Finally, as for RQ2R, in this case there is also no anomalous diffusion: for fixed T_1 and T_2 the heat flux is independent of L , as expected for 2-dimensional systems.

Experimental studies exist where the measurement of diffusivity is qualitatively compatible with our results (see e.g. [11], and Fig. 1 therein), even if the cylindrical model is obviously too simplified to reproduce details of real materials.

4 Conclusions and perspectives

The KQ dynamics we have introduced, in order to overcome restrictions intrinsic to standard microcanonical dynamics, proves highly efficient in the exploration of the whole range of temperatures intervals, providing a first dynamical insight in steady states of the cylindrical spin lattice with $T_1 < T_c < T_2$. In particular, we obtain a quantitative estimate of the dependence of diffusivity on the energy density, without any appeal to the Green-Kubo formula.

Once such an energy dependent diffusivity is assumed, the present analysis shows that heat transport follows the normal Fourier's law without anomalies (except maybe at the transition point, where diffusivity tends to 0 in the thermodynamic limit). In any case, the transition energy is comparable with the mean energy density corresponding to T_c in equilibrium theory. This confirms that there is a continuity between steady states very far from equilibrium and equilibrium states. The same continuity appears in the smoothness of the clustering process vs. L in the critical domain, resulting from the zooming procedure described at the end of Section 3.1. So far, however, this last observation is based only on visual inspection of configurations, and more refined analysis is required. The coexistence of different phases in the steady state opens up the problem of quantitative estimation of the relation between the phase transition inside the cylinder and the geometrical features of the surface sections perpendicular to x (e.g. with regard to the degree of clustering). In a future publication we shall deal with this problem using entropy based methods (e.g. metrization of partitions associated with the configurations) already used in different contexts (see for instance [12]).

As to the comparison with real materials, it would be interesting to introduce defects or other complications in the lattice, from small geometrical perturbations to a substantial alteration of the topological features (such as mean connectivity, fractality, breakdown of translational invariance or other symmetries), in order to have more direct control of the relevant features influencing heat transport. This kind of analysis is currently in progress.

Appendix A: The one dimensional case

For a one dimensional spin array, assume that the x th link in the configuration is $(++)$ (other cases may be

treated in the same way). This link has energy $e_x = 0$. There are four possible neighborhoods: (a) = $+(++)+$, (b) = $+(++)-$, (c) = $-(++)+$ and (d) = $-(++)-$. In the case (a), nothing can evolve. In both cases (b) and (c), we have exactly one possibility, namely that the evolution gives rise to (b') = $+(+-)-$ and to (c') = $-(-+)+$ respectively. Finally, there are two possibilities of evolution for (d), precisely (d') = $-(+--)- \equiv (-+)(--)$ and (d'') = $-(-+)- \equiv (--)(+-)$. Let us consider for example the configuration (b), such a configuration may also be read as (b) = $(++)(+-)$, i.e. the link x is connected with two links of energy $e_{x-1} = 0$ and $e_{x+1} = 1$. One can easily check that for any configuration the probability that the energy of the link x is increased by one unit is proportional to

$$P(e_x \rightarrow e_x + 1) \sim (e_{x-1} - e_x) + (e_{x+1} - e_x) \equiv \frac{\partial^2 e_x}{\partial x^2} \quad (10)$$

with the usually accepted continuous notation for discrete variables. The same relation holds also when the x th link is $(--)$. While for the cases $(+-)$ and $(-+)$ a similar relation (with opposite sign) describes the probability that the energy of the link is decreased by one unit. We conclude that in all cases, by linearity, for the averages we get

$$\frac{\partial \tilde{E}}{\partial t} = D \frac{\partial^2 \tilde{E}}{\partial x^2} \quad (11)$$

which is precisely Fourier's equation, with a constant diffusivity D , referring to the mean energy instead of

temperature. However, this microscopic approach cannot be generalized to the two dimensional lattice.

References

1. S. Lepri, R. Livi, A. Politi, Phys. Rep. **377**, 1 (2003)
2. K. Saito, S. Takesue, S. Miyashita, Phys. Rev. E **54**, 2404 (1996)
3. A.V. Sologubenko, K. Giannó, H.R. Ott, Phys. Rev. B **64**, 054412
4. A.V. Savin, G.P. Tsironis, X. Zotos, Phys. Rev. B **72**, 140402 (2005)
5. V. Lecomte, Z. Rácz, F. van Wijland, J. Stat. Mech., 02008 (2005)
6. K Saito, S. Takesue, S. Miyashita, Phys. Rev. E **59**, 2783 (1999)
7. L. Kadanoff, J. Swift, Phys. Rev. **165**, 310 (1968)
8. G.Y. Vichniac, Physica D **10**, 96 (1984)
9. Y. Pomeau, G.V. Vichniac, J. Phys. A: Math. Gen. **21**, 3297 (1988)
10. T. Toffoli, N. Margolus, *Cellular Automata Machines* (The MIT Press, Cambridge, 1987), pp. 185–205
11. M. Marinelli, F. Mercuri, U. Zammit, R. Pizzoferrato, F. Scudieri, Phys. Rev. B **49**, 4356 (1994)
12. M. Casartelli, L. Dall'Asta, E. Rastelli, S. Regina, J. Phys. A: Math. Gen. **37**, 11731 (2004)